A Theoretical Study of Dibenzothiophene Absorbed on Open-Ended Carbon Nanotubes

B. Gómez* and J. M. Martínez-Magadán

Programa de Ingeniería Molecular, Instituto Mexicano del Petróleo, Lázaro Cárdenas 152, Col. San Bartolo de Atepehuacan, Gustavo A. Madero, México D. F. 07730, México

Received: February 3, 2005; In Final Form: June 13, 2005

The (7,7) and (10,5) carbon nanotubes were studied in the context of the Density Functional Theory (DFT) within a generalized gradient approximation (GGA). The Becke's exchange functional along with the correlation functional of Lee, Yang, and Parr (BLYP) were used with the DZVP basis set aided via auxiliary functions for the electron density. In both materials, the global indexes were calculated from the optimized structure with Kopmanns' theorem. The energy values calculated for the physisorption and chemisorption processes suggested that the physisorption process is more likely to occur for the (7,7) than for the (10,5) carbon nanotube, as well as for the achiral than chiral structure for both nanotubes and for both surface phenomena. This effect may be ascribed to the more homogeneous distribution of molecular orbital for the achiral carbon nanotube, which seems to be supported by the DOS calculations.

Introduction

The discovery of nanotubes by Iijima[1] in 1991 gave birth to a large number of scientific investigations. The mechanical, chemical, and electrical properties of these new materials were eagerly studied all over the world. As carbon nanotubes show a cylindrical shape, research efforts have concentrated on the possibility of controlling alignment, diameters, and lengths.[2] Much attention has been focused on the exciting possibilities of one-dimensional (1D) and two-dimensional (2D) adsorption of gases on bundles of single-wall carbon nanotubes (SWCNTs),[3,4] so that many theoretical and experimental studies on these topics have been reported.[3,5] Classical and path integral molecular simulations were used to study the physisorption of hydrogen, helium, neon, nitrogen, argon, and methane in cylindrical pores, SWCNTs, and bundles of SWCNT for a range of pressures, temperatures, tube radii, and bundle structures.[6] There is currently a considerable interest in the functionalization of carbon nanotubes, one motivation being to increase their very low solubility in both aqueous and organic solvents.[7] Both covalent and noncovalent interactions have been reported,[8] including hydrogenation, oxidation, ozonization, 1,3-dipolar cycloaddition, fluorination, amidization, attachment of polymers, and immobilization of proteins and other biomolecules. Tournus et al.[8b] have performed studies about the adsorption of benzene molecules on carbon nanotubes. Recently, carbon nanotubes have been employed as supports for some catalysts, which are commonly used to remove molecules that contain sulfur atoms in its structure.[8c]

Sulfur is present in every stage of oil production and refining so that large economic resources are invested on removal processes. Additionally, this element acts as a pollutant so that sulfur emissions to the environment are increasingly restricted. The oil industry is quite interested in testing new technology to eliminate sulfur present in hydrocarbons. At present, the hydrodesulfurization process exists in every plant as a reduction process to remove sulfur compounds. However, only a few investigations are aimed at the process of oxidative elimination, and it is therefore urgent to find new mechanisms of sulfur removal in oil process currents. The exotic properties of carbon nanotubes can offer new possibilities, which may range from sulfur elimination to reduction and oxidation reactions of sulfur compounds.

Density Functional Theory (DFT)[9] has been successful in providing insights into the chemical reactivity and selectivity of molecules based on their global and local reactivity indexes. The global index includes molecule electronegativity[10] (χ) and hardness[11] (η) while the local index includes the Fukui function[12] ($f(r)$) and local softness[13] ($s(r)$). Pauling[14] introduced the concept of electronegativity as "the power of an atom in a molecule to attract electrons to itself". The concept of hardness was put forward by Pearson in his hard−soft acids and bases (HSAB) principle, which states that[15] "hard likes hard and soft likes soft". Another hardness-based principle is the maximum hardness principle[16−20] (MHP), which states that[17] "there seems to be a rule of nature that molecules arrange themselves so as to be as hard as possible". The MHP has been found to be successful[19] in analyzing molecular vibration and internal rotation, different types of chemical reactions, aromaticity, clusters with a magic number of atoms, extra stability of a closed-shell species, dynamical problems, and electronic excitation in atoms[21] and molecules.[22]

For an N-electron system with a total energy (E) and external potential ($v(\vec{r})$), electronegativity (χ) and hardness (η) are respectively defined as the following first-order[23] and second-order[24] derivatives:

$$\chi = -\left(\frac{\partial E}{\partial N}\right)_{v(\vec{r})} = -\mu \tag{1}$$

and

$$\eta = \frac{1}{2}\left(\frac{\partial^2 E}{\partial N^2}\right)_{v(\vec{r})} \tag{2}$$

The chemical potential (μ) is defined as the negative of the electronegativity. In addition the global softness is given by the

* Address correspondence to this author. Phone: (+5255)-9175-8425. Fax: (+5255)-9175-6239. E-mail: bgomez@imp.mx.

10.1021/jp050615o CCC: $30.25
Published on Web 07/16/2005

inverse of hardness:[9]

$$S = \frac{1}{\eta} \tag{3}$$

Recently, Parr et al.[25] have introduced an electrophilicity index (w) defined as:

$$w = \frac{\mu^2}{2\eta} \tag{4}$$

This is proposed as a measure of the electrophilic power of a molecule.

The total density of states (DOS) is an indicator of what could happen in the different molecular levels of energy; its analysis offers suitable information about the electronic population in the interior of a molecule or molecular complex.

In this paper, a theoretical study about adsorption (physisorption and chemisorption) of dibenzothiophene upon two nanomaterials was carried out. A (7,7) carbon nanotube (achiral) with 224 carbon atoms and 28 hydrogen atoms and a (10,5) carbon nanotube (chiral) with 280 carbon atoms and 30 hydrogen atoms were studied. Index calculations were made completely ab initio, and in this way the indexes of global reactivity were calculated from the values of the frontier orbitals. The carbon nanotubes were constructed by using its chiral vectors. For the total density of states, the vector of the eigenvalues from the ab Initio calculations of the optimized molecules was included.

Computational Details

The interaction between the dibenzothiophene molecule and the (7,7) carbon nanotube (achiral), as well as (10,5) carbon nanotube (chiral), has been studied by the density functional theory in the generalized gradient approximation (GGA) through the Becke[27] exchange functional (B) and the Lee, Yang, and Parr[28] (LYP) correlation functional. All structures were optimized with a DZVP[26] basis set in combination with auxiliary functions (GEN-A2*) for the electron density. The single point calculations (SP) were done in all cases with the BLYP/DZVP level theory for optimized molecules.

The study was done for the physisorption (the process whereby the molecule is stabilized on the surface without any type of chemical bonding taking place between the molecule and the carbon nanotube) and for the chemisorption process (the process whereby chemical bonding comes about due to changes in the hybridization of the carbon nanotube (sp^2 to sp^3) with the presence of the sulfur atom of the dibenzothiophene molecule, which undergoes an expansion in its valence level).

Chemical potential (μ) and hardness (η) were calculated as half the energy of the Fermi level (E_{HOMO}) plus the first eigenvalue of the valence band (E_{LUMO}), and half the energy of the valence band (E_{LUMO}) less the energy of the Fermi level (E_{HOMO}), respectively:

$$\mu = \frac{E_{HOMO} + E_{LUMO}}{2}; \qquad \eta = \frac{E_{LUMO} - E_{HOMO}}{2} \tag{5}$$

These definitions were derived from eqs 1 and 2 by the finite difference approximation, in addition to Kopmanns' theorem.[29]

The total density of states was calculated from the eigenvalues generated by single point calculations, as follows:

$$\mathrm{DOS}(E) = \sum_{i=1}^{N} \mathrm{occ}(i) \exp[-(E - C_i)^2] \tag{6}$$

where N is the number of orbitals, occ(i) the number of occupation, and C_i the vector of eigenvalues of the molecular orbitals. In all graphs the Fermi level was centered on the 0 value.

All quantum mechanics calculations were solved with the deMon[30] computational package. The visualization of results for the single point calculations was done with Molden[31] and GausView 3.07.[32]

Results and Discussion

From the primary symmetry classification, a carbon nanotube may have either achiral (symmorphic) or chiral (nonsymmorphic)[33] structures. An achiral carbon nanotube is defined as a carbon nanotube whose mirror image has an identical structure to the original one. There are only two types of achiral nanotubes: armchair and zigzag. Chiral nanotubes exhibit a spiral symmetry whose mirror image cannot be superposed onto the original one. The zigzag structure would require a larger number of carbon atoms to reach the same nanodiameter, which involves longer calculation time. A carbon nanotube of each type (achiral and chiral) was studied in this work considering that both have an average diameter within 0.7−2.0 nm for single wall carbon nanotubes.[33]

Figure 1 shows the optimized structures of the (7,7) and (10,5) carbon nanotubes, as well as the structures in the stationary states for the physisorption and chemisorption processes, respectively. It was determined that the average bond length between carbon atoms is 1.423 Å for both carbon nanotubes, which is in agreement with the experimental value of 1.44 Å reported elsewhere.[33] The dangling bonds were filled with hydrogen atoms, and an average bond length of 1.098 Å was obtained in both cases of optimized geometry. These results were obtained from the optimized structures of the carbon nanotubes without interacting with the dibenzothiophene molecule, as is showed in Figure 1a,b.

The highest occupied molecular orbital of valence band (HOMO) and the lowest unoccupied molecular orbital of a conduction band (LUMO), as well as the DOS for the (7,7) carbon nanotube, are presented in Figure 2a−c, and that for the (10,5) in Figure 3a−c. The eigenvalues from the final single point calculations were considered in order to generate a graph of the DOS using eq 6; these graphs are depicted in Figures 2c and 3c. From the optimized geometry of carbon nanotubes one can see that the (7,7) and (10,5) carbon nanotubes (Figure 1a,b) have a tubular diameter of approximately 9.713 and 10.008 Å, respectively; the (7,7) is 0.295 Å smaller than the (10,5) carbon nanotube. From the results of eq 6, it can observed that the DOS for the (7,7) carbon nanotube behaves like a metallic system displaying a small difference between the Fermi energy level and conduction band of 0.39 eV. This theoretical result is in complete agreement with the experimental determinations reported in the literature for the armchair structure of the achiral-type carbon nanotubes.[33] For the (10,5) carbon nanotube, Figure 3c shows a difference of 0.50 eV between the Fermi level and the conduction band. This carbon nanotube also displays a metallic behavior, which is consistent with that observed for some nonsymmorphic carbon nanotubes.[33] If the relationship of gap values is considered for the (7,7) and (10,5) carbon nanotubes, the first one presents a more metallic character by approximately 0.11 eV.

Frequencies were calculated for the optimized structure of the dibenzothiophene molecule to confirm that it corresponds to the ground state of this molecule. Non-negative value in the elements of the Hessian matrix was found since non-imaginary

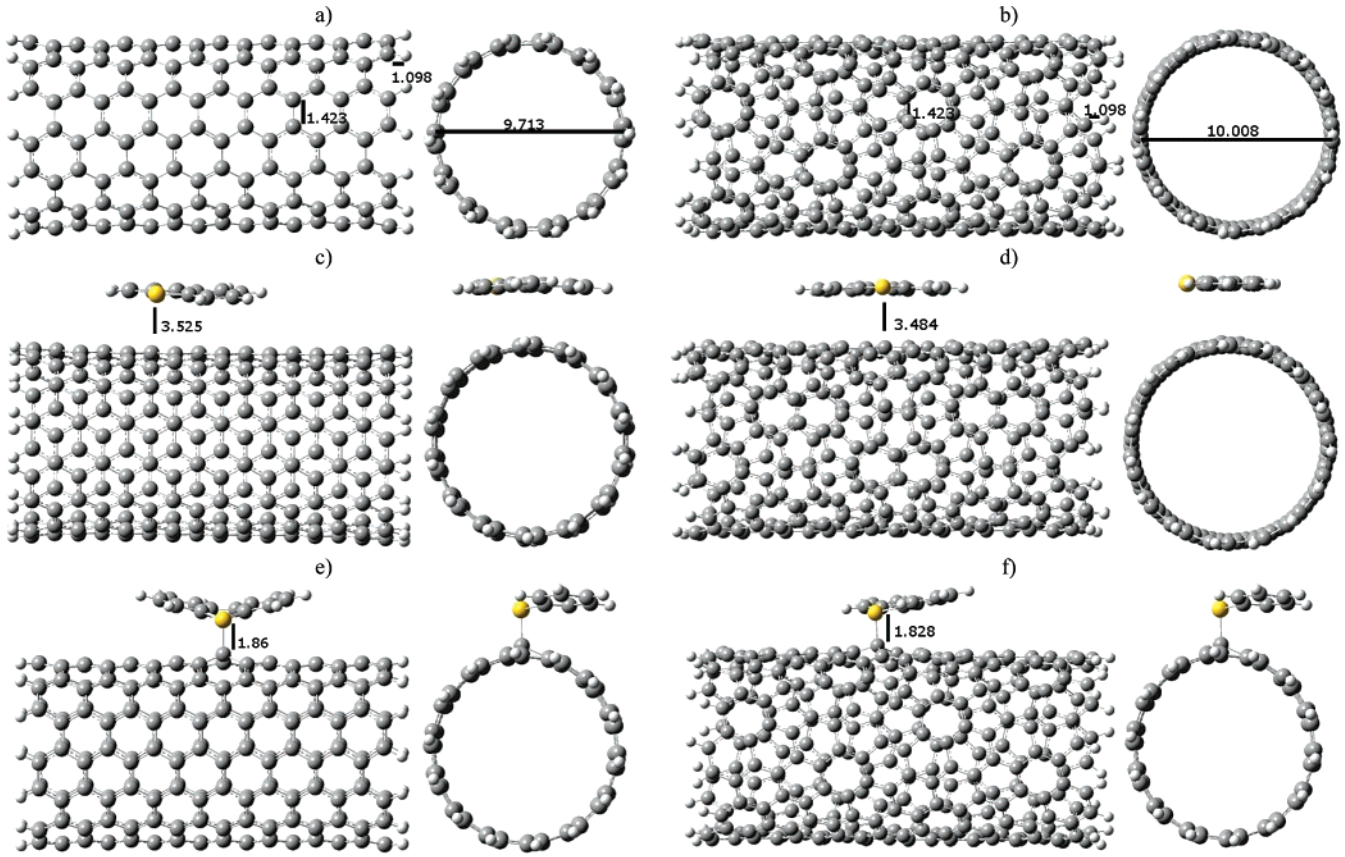

Figure 1. The optimized geometries for (a) the (7,7) carbon nanotube, (b) the (10,5) carbon nanotube, (c) the dibenzothiophene molecule over the (7,7) carbon nanotube in the physisorption process, (d) the dibenzothiophene molecule over the (10,5) carbon nanotube in the physisorption process, (e) the dibenzothiophene molecule over the (7,7) carbon nanotube in the chemisorption process, and (f) the dibenzothiophene molecule over the (10,5) carbon nanotube in the chemisorption process.

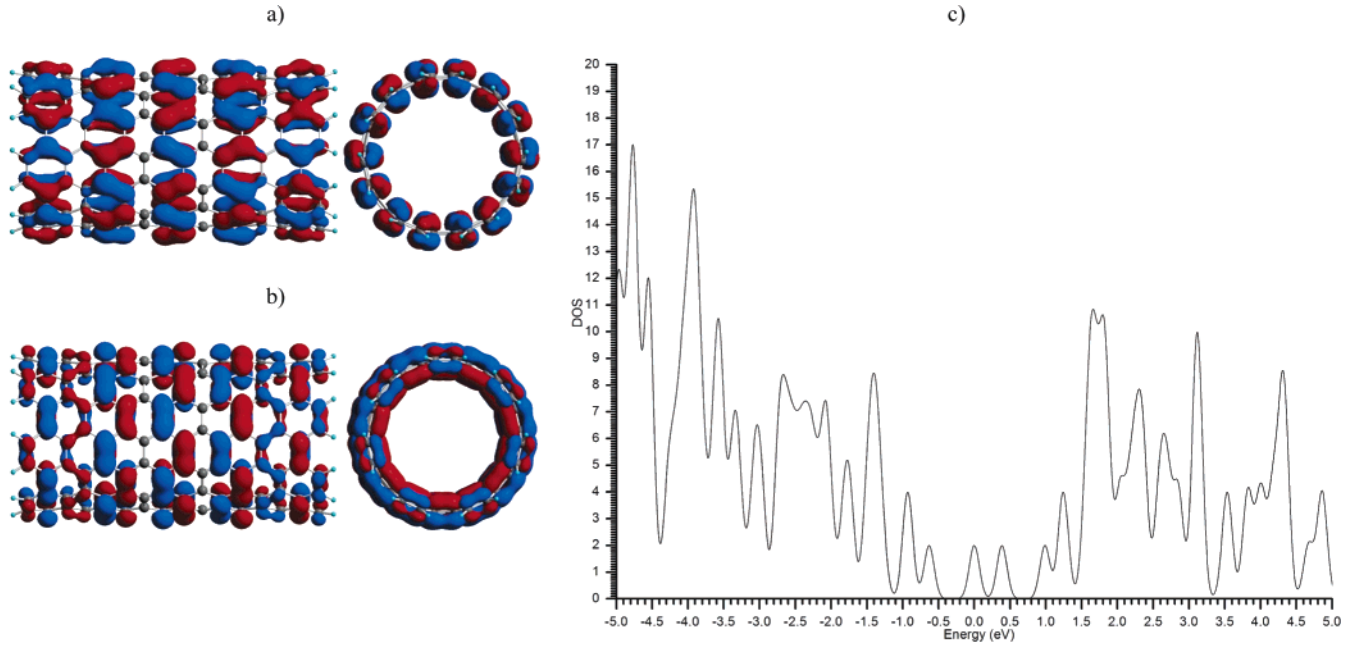

Figure 2. (a) The HOMO of the (7,7) carbon nanotube with isosurface values of 0.02, (b) the LUMO of the (7,7) carbon nanotube with isosurface values of 0.02, and (c) the DOS graphs for the (7,7) carbon nanotube with a Gaussian bandwidth equal to 0.1.

frequency was identified. In the HOMO, the sulfur atom has the highest contribution (Figure 4a), whereas the LUMO displays a great contribution from the electronic pairs of benzene rings. The thiophene entity (Figure 4b) favors the benzene ring interactions. The global indexes of reactivity in the context of density functional theory are presented in Table 1. The dibenzothiophene molecule displayed the highest value of hardness (1.66 eV), which is related to the great stability of this molecule. The DOS of dibenzothiophene is shown in Figure 4c, and the difference of energy between the HOMO and LUMO levels can be observed; the gap has a value of 3.32 eV. The dibenzothiophene molecule behaved like a very stable molecule due

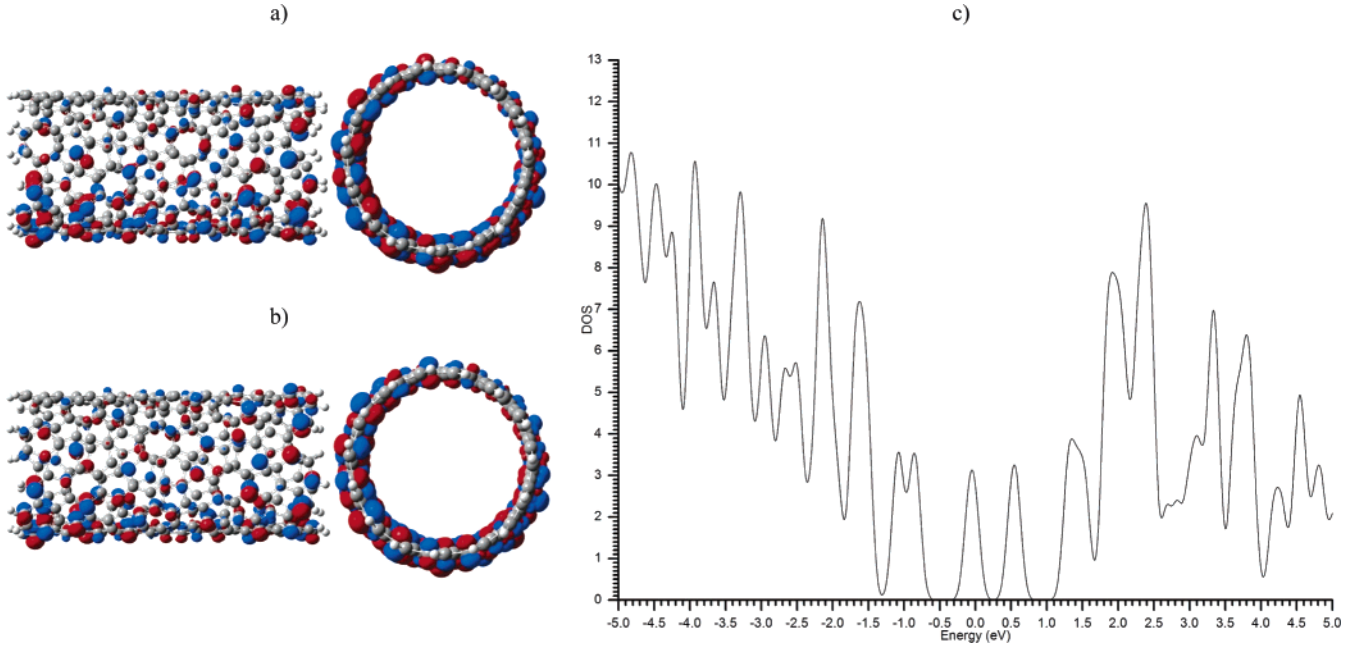

Figure 3. (a) The HOMO of the (10,5) carbon nanotube with isosurface values of 0.02, (b) the LUMO of the (10,5) carbon nanotube with isosurface values of 0.02, and (c) the DOS graphs for the (10,5) carbon nanotube with a Gaussian bandwidth of 0.1.

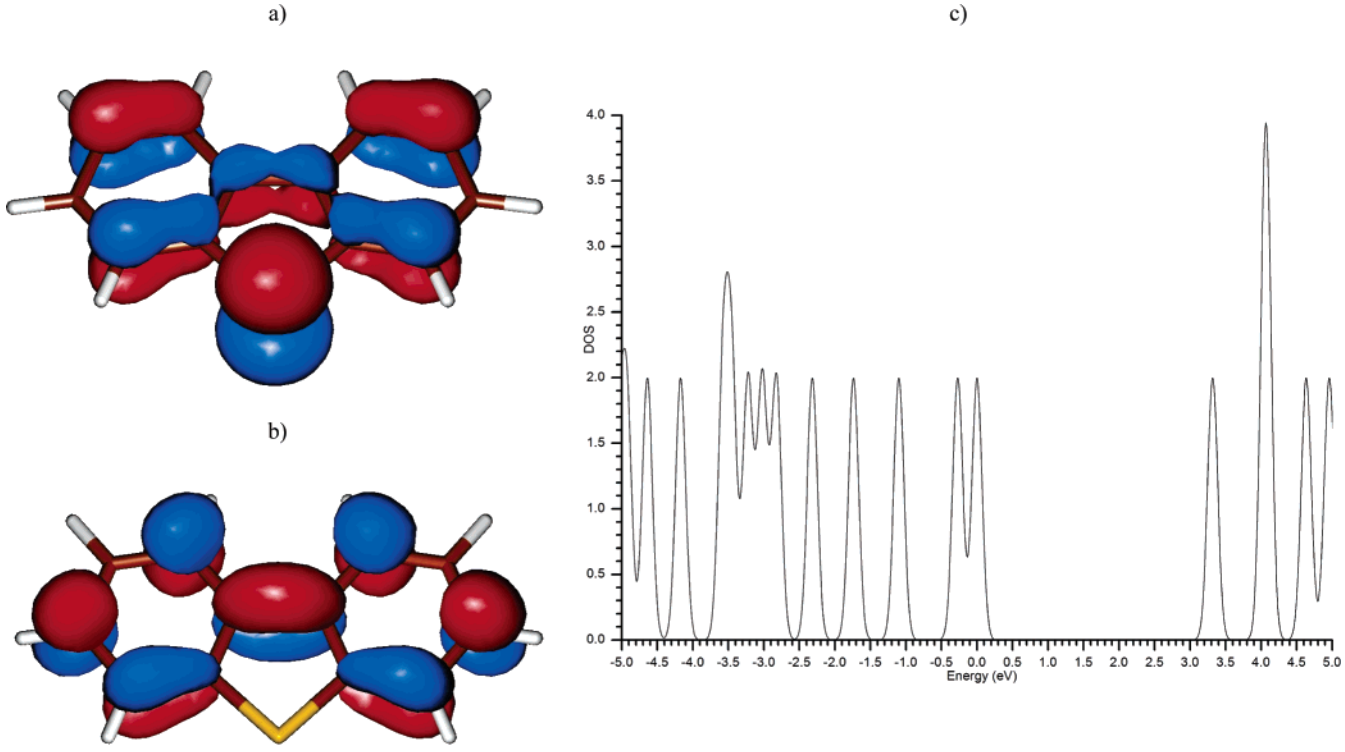

Figure 4. (a) The HOMO of the dibenzothiophene molecule with isosurface values of 0.02, (b) the LUMO of the dibenzothiophene molecule with isosurface values of 0.02, and (c) the DOS graphs for the dibenzothiophene molecule with a Gaussian bandwidth of 0.1.

to the difference in the energy of its frontier orbitals. The high coefficient of wave function for the sulfur atom in the HOMO indicates the large probability that the molecule can undergo an electrophilic attack.

The physisorption process for the (7,7) carbon nanotube occurred when the dibenzothiophene molecule was located at a distance of 3.525 Å (Figure 1c), namely that between the sulfur atom of the dibenzothiophene and the closest carbon atom over the surface of the carbon nanotube. It is observed from Figure 5, parts a and b, that neither the HOMO nor the LUMO present a large contribution form the dibenzothiophene molecule. The DOS graph (Figure 5c) is clear in the sense that below the Fermi level, the electronic states were modified between −3.0 and −1.5 eV; in the case of the conduction band a more significant modification occurred between 3.7 and 4.5 eV. However, the gap was not modified, as can be seen from the hardness values (Table 1), which may imply that the physisorption process does not modify the molecular reactivity but alters the internal orbital energy. Moreover, if the electrophilicity values (ω) are considered, the (7,7) carbon nanotube diminishes its capacity to attract electrons when the dibenzothiophene molecule undergoes the physisorption process.

TABLE 1. Total Energy (E_T),[a] Chemical Potential (μ),[b] Hardness (η),[b] Softness (S),[c] Electrophilicity (ω),[b] Physisorption Energy (ΔE_{Ph}),[d] and Chemisorption Energy (ΔE_{Ch})[d] for Physisorption and Chemisorption Processes of the Dibenzothiophene (DBT) Over the (7,7) and (10,5) Carbon Nanotubes

species	E_T	μ	η	S	ω	ΔE_{Ph}	ΔE_{Ch}
DBT	−860.1143	-3.505	1.659	0.603	1.852		
(7,7)[e]	−5884.1343	-3.632	0.193	5.176	17.074		
(10,5)[f]	−5732.0690	-3.409	0.249	4.021	11.678		
(7,7)-DBT[g]	−6744.1998	-3.598	0.195	5.129	16.604	30.59	
(10,5)-DBT[h]	−6592.0566	-3.393	0.249	4.023	11.577	79.44	
(7,7)-DBT[i]	-6744.0412	-3.536	0.192	5.220	16.316		130.15
(10,5)-DBT[j]	-6591.9406	-3.185	0.207	4.823	12.229		152.26

[a] In atomic units. [b] In eV. [c] In 1/eV. [d] In kcal/mol. [e] The (7,7) carbon nanotube. [f] The (10,5) carbon nanotube. [g] Super molecule of the (7,7) carbon nanotube with the dibenzothiophene during the physisorption process. [h] Super molecule of the (10,5) carbon nanotube with the dibenzothiophene during the physisorption process. [i] Super molecule of the (7,7) carbon nanotube with the dibenzothiophene during the chemisorption process. [j] Super molecule of the (10,5) carbon nanotube with the dibenzothiophene during the chemisorption process.

For the (10,5) carbon nanotube, the intermolecular distance between sulfur and carbon atoms for the physisorption process was 3.484 Å (Figure 1d), which is slightly smaller than that of the (7,7) carbon nanotube. The HOMO, LUMO, and DOS for the (10,5) carbon nanotube are presented in the Figure 6, parts a, b, and c, respectively. Likewise, it is not observed as an important variation of the Fermi level and conduction band energy when DOS of the carbon nanotube is compared with and without the dibenzothiophene molecule. The values of hardness and softness are quite similar when carbon nanotube interacts with the dibenzothiophene molecule, and when this molecule is absent. On the contrary, the chemical potential and electrophilicity vary, so that the capacity to attract electrons by part of the (10,5) carbon nanotube diminishes as it occurred for the (7,7) carbon nanotube.

The chemisorption process for the (7,7) carbon nanotube took place when the dibenzothiophene molecule was linked to the surface at a distance of 1.86 Å (Figure 1e). The sulfur atom of the dibenzothiophene molecule and the carbon atom of the nanotube surface are joined by a σ bond. This distance is slightly larger than that between the carbon and sulfur atoms in the dibenzothiophene molecule, which is 1.784 Å. HOMO (Figure 7a) presents a contribution only over the sulfur atom of the dibenzothiophene molecule meanwhile the benzene rings contribution is absent, if they are compared with HOMO of the dibenzothiophene molecule alone. However, in the LUMO (Figure 7b) this contribution is not observed; this is probably because the sulfur atom behaved like a nucleophilic center in relation to the (7,7) carbon nanotube, when the sulfur atom expands its shell valence. It is observed (Figure 7a,b) that a chemical bond was formed by means of a retrodonation via the sulfur atom. Additionally, the dibenzothiophene molecule tends to distort its molecular plane by pushing the rings of benzene in the opposite direction to the bond formed with the (7,7) carbon nanotube. From the graph of DOS (Figure 7c), it is worth noticing that the Fermi level is slightly degenerated and below this the DOS was modified. The conduction band underwent stronger modifications in the region between 0.8 and 4.5 eV. The hardness value of the (7,7) carbon nanotube bonded to the dibenzothiophene molecule remained constant when it was compared to that of the (7,7) carbon nanotube alone. Both electrophilicity and chemical potential indexes changed as in the physisorption process; the carbon nanotube that was bonded to the dibenzothiophene molecule lost its capacity to attract electrons, which is consistent with the DOS. Although the value of the hardness did not change, the eigenvalues of the HOMO and LUMO were modified.

For the (10,5) carbon nanotube, the bond length between the sulfur atom of the dibenzothiophene molecule and the carbon atom of the surface of the carbon nanotube is 1.828 Å (Figure 1f). This distance is smaller than that of the (7,7) carbon nanotube for the bond length of the C−S atoms with the dibenzothiophene molecule. The orientation of the dibenzothiophene molecule is parallel to the translation vector and with a slight rotation toward the chiral axis. The dibenzothiophene molecule has a contribution at the HOMO (Figure 8a); the zone where the sulfur atom is bonded with the carbon atom has a greater contribution in this molecular orbital. In the LUMO (Figure 8b), the dibenzothiophene molecule does not present any contribution; the reactivity is transferred funda-

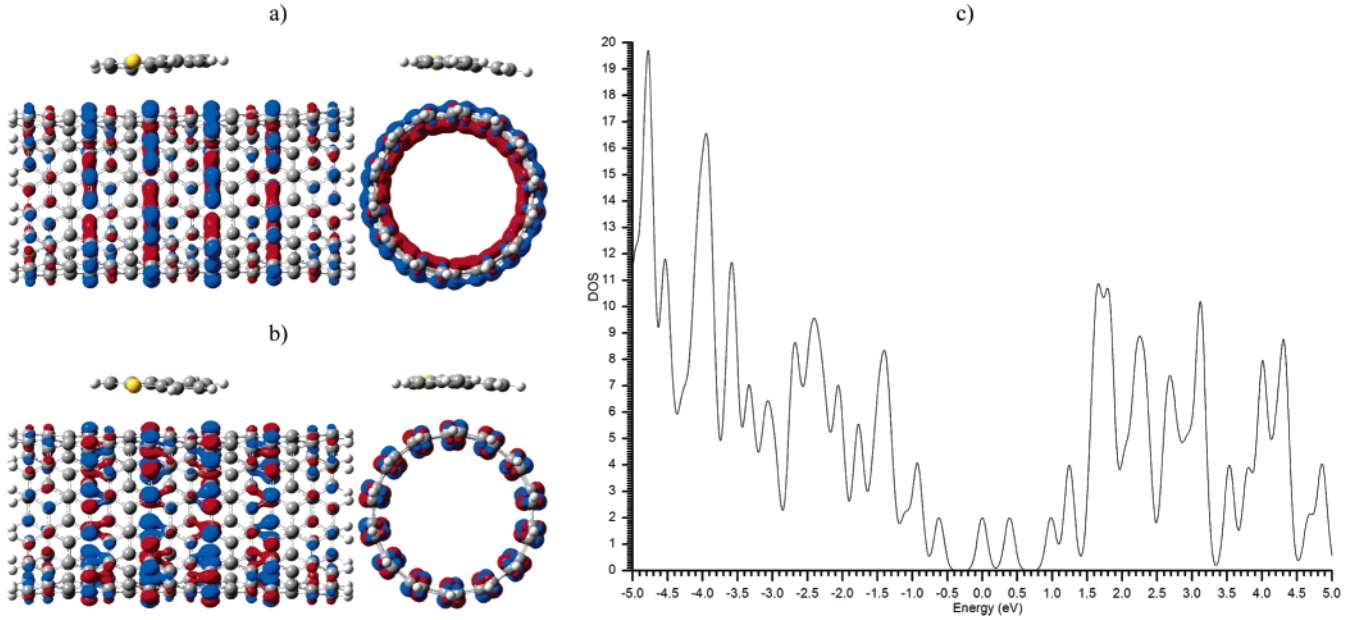

Figure 5. (a) The HOMO with isosurface values of 0.02, (b) the LUMO with isosurface values of 0.02, and (c) the DOS graphs for the dibenzothiophene molecule over the (7,7) carbon nanotube, during the physisorption process with a Gaussian bandwidth of 0.1.

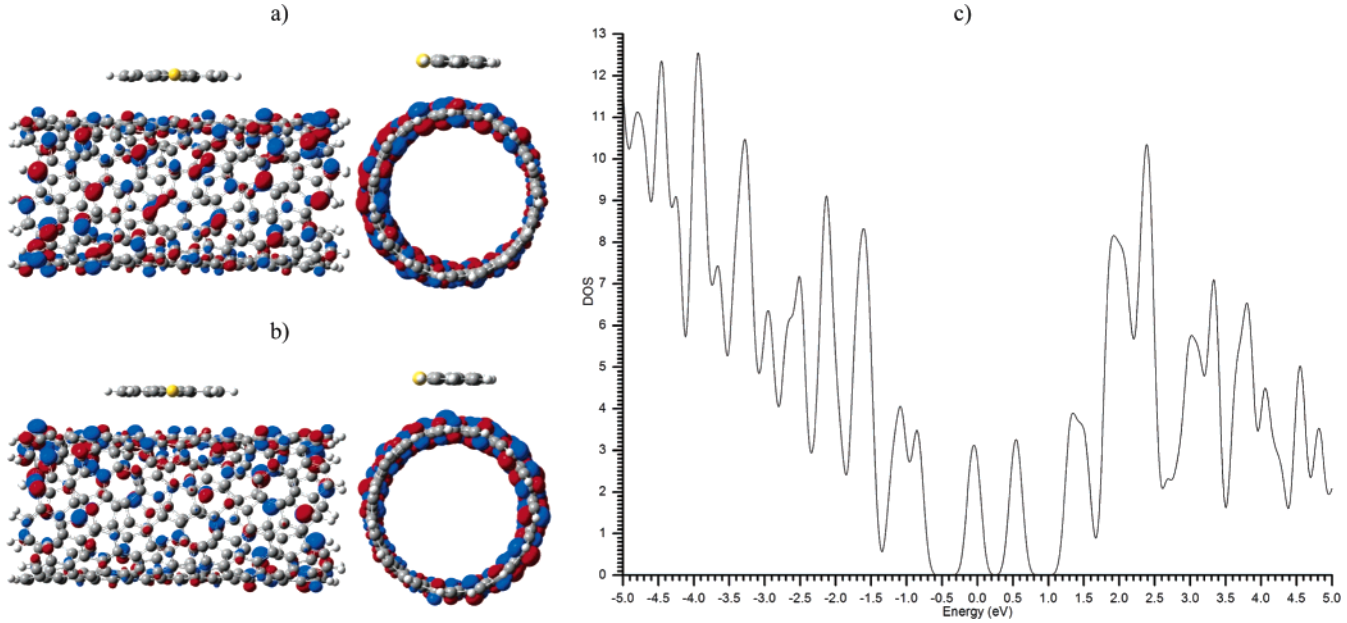

Figure 6. (a) The HOMO with isosurface values of 0.02, (b) the LUMO with isosurface values of 0.02, and (c) the DOS graphs for the dibenzothiophene molecule over the (10,5) carbon nanotube, during the physisorption process with a Gaussian bandwidth of 0.1.

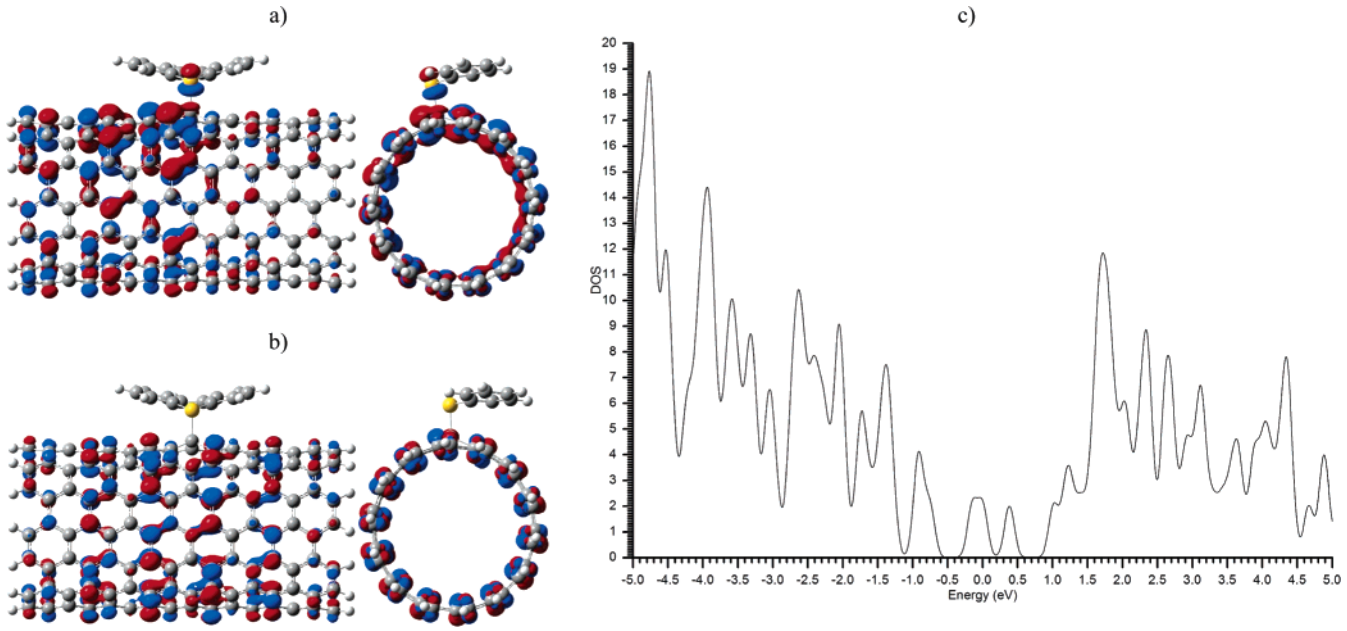

Figure 7. (a) The HOMO with isosurface values of 0.02, (b) the LUMO with isosurface values of 0.02, and (c) the DOS graphs for the dibenzothiophene molecule over the (7,7) carbon nanotube, during the chemisorption process with a Gaussian bandwidth of 0.1.

mentally toward the terminal carbons of the (10,5) carbon nanotube. The DOS is presented in Figure 8c, which shows that the Fermi level has been strongly modified, especially in the frontier zone between −1.5 and 0 eV. The conduction band also changed between 0.4 and 5.0 eV, and the LUMO remained approximately constant because it underwent a variation of 0.18 eV. This can provide a better understanding of why the carbon nanotube reactivity is higher at the carbon nanotube ends. The reactivity of the (10,5) carbon nanotube that was bonded to the dibenzothiophene molecule increased as well as its metallic character, which can be clearly observed from the hardness and softness values. The capacity to attract electrons was increased in the species bonded (the carbon nanotube and the dibenzothiophene molecule) as observed from the electrophilicity and chemical potential values.

The energy for physisorption process of the (7,7) and (10,5) carbon nanotubes was 30.59 (1.33 eV) and 79.44 kcal/mol (3.45 eV), respectively, while that for the chemisorption process were 130.15 (5.64 eV) and 152.26 kcal/mol (6.60 eV), respectively. Both results have an acceptable magnitude when they are compared to those obtained from the interaction of the thiophene molecule with metallic surfaces.[34] The physisorption process is more likely to occur for the (7,7) than for the (10,5) carbon nanotube, for both surface phenomena. Apparently, the more homogeneous distribution of the molecular orbital for the (7,7) carbon nanotube in its isolated form favors the molecular interaction over the carbon nanotube surface (Figure 2a,b).

The electrostatic potential mapped with electron density was calculated by using an isosurface value of 0.02 for the carbon nanotubes with and without the dibenzothiophene molecule. In Figure 9a,b, the electrostatic potential for (7,7) and (10,5) carbon nanotubes without the dibenzothiophene molecule is displayed. It is important to note that the chiral (10,5) carbon nanotube has a more positive electrostatic potential in the center of the

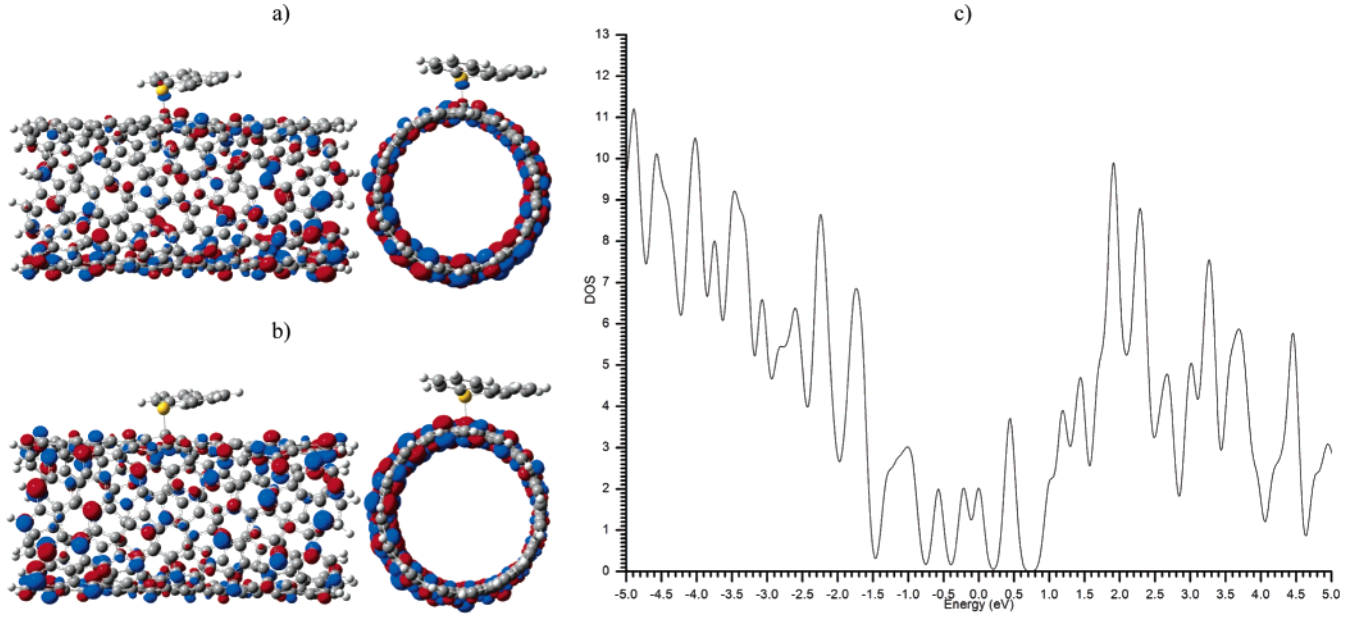

Figure 8. (a) The HOMO with isosurface values of 0.02, (b) the LUMO with isosurface values of 0.02, and (c) the DOS graphs for the dibenzothiophene molecule over the (10,5) carbon nanotube, during the chemisorption process with a Gaussian bandwidth of 0.1.

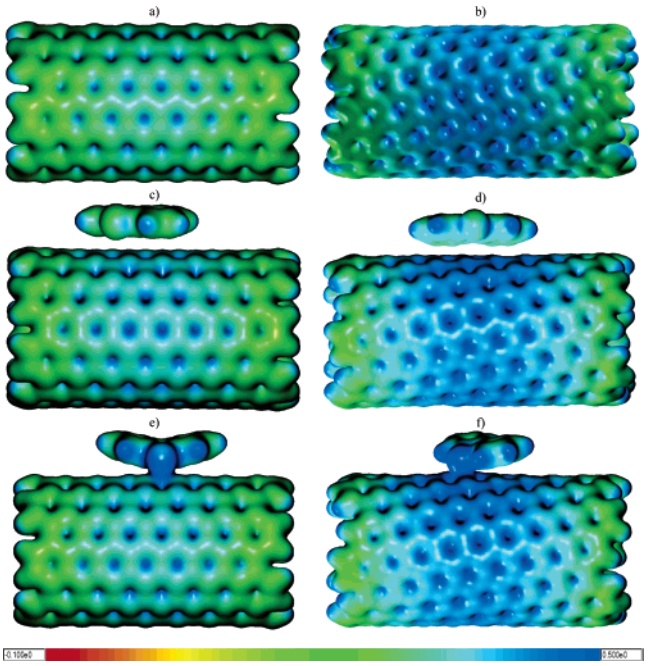

Figure 9. The electrostatic potential for: (a) the (7,7) carbon nanotube, (b) the (10,5) carbon nanotube, (c) the dibenzothiophene molecule over the (7,7) carbon nanotube in the physisorption process, (d) the dibenzothiophene molecule over the (10,5) carbon nanotube in the physisorption process, (e) the dibenzothiophene molecule over the (7,7) carbon nanotube in the chemisorption process, and (f) the dibenzothiophene molecule over the (10,5) carbon nanotube in the chemisorption process.

nanotube than that of the achiral (7,7) carbon nanotube. In Figure 9c,d, the dibenzothiophene molecule over the surface of the carbon nanotubes for the physisorption process is shown; the electrostatic potential was modified significantly in the central region of the carbon nanotubes. In Figure 9e,f, the electrostatic potential for the (7,7) and (10,5) carbon nanotubes for the chemisorption process is illustrated. In both cases, the sulfur atom presented a modification; however, this modification was larger for the (10,5) than for the (7,7) carbon nanotube, which is probably due to the geometrical modifications that the dibenzothiophene molecule undergo.

Concluding Remarks

The (7,7) and (10,5) carbon nanotubes with 224 and 280 atoms, respectively, were characterized in their ground state, and also when they are interacting with the dibenzothiophene molecule in the physisorption and chemisorption processes. The calculations were done with all electrons (ab initio), by means of the density functional theory (BLYP) and the DZVP basis set. The energy for the physisorption process of the (7,7) and (10,5) carbon nanotubes was 30.59 (1.33 eV) and 79.44 kcal/mol (3.45 eV), respectively, while for the chemisorption process it was 130.15 (5.64 eV) and 152.26 kcal/mol (6.60 eV), respectively. Accordingly, the physisorption process is more likely to occur for the (7,7) than for the (10,5) carbon nanotube, as well as for the achiral than for the chiral structure, for both nanotubes and for both surface phenomena. Apparently, the more homogeneous distribution of molecular orbital for the (7,7) carbon nanotube in its isolated form favors the molecular interaction over the carbon nanotube surface. In the case of the chiral carbon nanotube, the axis C_{2v} of the dibenzothiophene molecule presented the same direction as the chiral vector of the carbon nanotube. The DOS clearly shows that in the physisorption and chemisorption processes, the states below the Fermi level and over the conduction band were modified when the dibenzothiophene molecule approached the carbon nanotube; this energy change was higher for the chemisorption compared to the physisorption process, but in the former it was more evident as observed in the DOS graph.

Acknowledgment. B.G. gratefully acknowledges the Instituto Mexicano del Petróleo (IMP) for granting a postdoctoral position in the Programa de Ingeniería Molecular. Acknowledgments are also due to the Sistema Nacional de Investigadores (SNI-CONACYT) for a complementary grant. The authors also thank Dr. M. A. Dominguez for his valuable collaboration in the Results and Discussion section.

References and Notes

(1) (a) Iijima, S. *Nature* **1991**, *354*, 56. (b) Iijima, S.; Ichihashi, T. *Nature* **1993**, *364*, 737.

(2) (a) Bandow, S.; Asaka, S.; Saito, Y.; Rao, A. M.; Gregorian, L.; Richter, E.; Eklund, P. C. *Phys. Rev. Lett.* **1998**, *80*, 3779. (b) Venema, L.

C.; Wildöer, J. W. G.; Temminck, H. L. J.; Dekker, C.; Rinzler, A. G.; Smalley, R. E. *Appl. Phys. Lett.* **1997**, *75*, 2629. (c) Xu, D.; Guo, G.; et al. *Appl. Phys. Lett*. **1999**, *71*, 481. (d) Jost, O.; Gorbunov, A. A.; Pompe, W.; et al. *Appl. Phys. Lett.* **1999**, *75*, 2217.

(3) (a) Rols, S.; Johnson, M. R.; Zeppenfeld, P.; et al. *Phys. Rev. B* **2005**, *71*, 155411. (b) Clabi, M. M.; Cole, M. W.; Gatica, S. M.; Bonja, M. J.; Stan, G. *Rev. Mod. Phys*. **2001**, *73*, 875. (c) Lu, A. J.; Pan, B. C. *Phys. Rev. B* **2005**, *71*, 165416. (d) Zheng, Q. R.; Gu, A. Z.; Lu, X. S.; et al. *J. Supercrit. Fluids* **2005**, *34*, 71.

(4) (a) Muris, M.; Dufau, N.; Bienfait, M.; Dupont-Pavlovsky, N.; Grillet, Y.; Palmari, J. P. *Lagmuir* **2000**, *16*, 7019. (b) Muris, M.; Bienfait, M.; Zeppenfeld, P.; Dupont-Pavlovsky, N.; Johnson, M.; Vilches, O. E.; Wilson, T. *Appl. Phys. Lett.* **2002**, *74*, S1293. (c) Winson, T.; Tyburski, A.; DePies, M. R.; Vilches, O. E.; Becquet, D.; Bienfait, M. *J. Low Temp. Phys.* **2002**, *126*, 403. (d) Fujiwara, A.; Ishii, K.; Suematsu, H.; Kataura, H.; Maniwa. Y.; Suzuki, S.; Achiba, Y. *Chem. Phys. Lett.* **2001**, *336*, 205. (e) Mirus, M.; Dupont-Pavlovsky, N.; Bienfait, M.; Zeppenfeld, P. *Surf. Sci.* **2001**, *492*, 67. (f) Talapatra, S.; Migone, A. D. *Phys. Rev. Lett.* **2001**, *87*, 206106. (g) Talapatra, S.; Migone, A. D. *Phys. Rev. B* **2002**, *65*, 045416.

(5) (a) Talapatra, S.; Zambano, Z.; Weber, S. E.; Migone, A. D. *Phys. Rev. Lett*. **2000**, *85*, 138. (b) Tiezer, W.; Hallock, R. B.; Dujardin, E.; Ebbesen, T. W. *Phys. Rev. Lett*. **1999**, *82*, 5305. (c) Tiezer, W.; Hallock, R. B.; Dujardin, E.; Ebbesen, T. W. *Phys. Rev. Lett*. **2000**, *84*, 1844(E). (d) Kahng, Y. H.; Hallock, R. B.; Dujardin, E.; Ebbesen, T. W. *J. Low Temp. Phys*. **2002**, *126*, 223. (e) Boninsegni, M.; Lee, S. Y.; Crespi, V. H. *Phys. Rev. Lett*. **2001**, *73*, 857. (f) Cole, M. W.; Crespi, V. H.; Stan, G.; Ebner Hartman, J. M.; Moroni, S.; Boninsegni, M. *Phys. Rev. Lett.* **2000**, *84*, 3883. (g) Gatica, S. M.; Bojan, M. J.; Stan, G.; Cole, M. W. *J. Chem. Phys*. **2001**, *114*, 3765. (h) Stan, G.; Bojan, M. J.; Curtarolo, S.; Gatica, S. M.; Cole, M. W. *Phys. Rev. B* **2000**, *62*, 2173. (i) Siber, A. *Phys. Rev. B* **2002**, *66*, 205406. (j) Siber, A.; Buljan, H. *Phys. Rev. B* **2002**, *66*, 075415. (k) Silber, A. *Phys. Rev. B* **2002**, *66*, 235414.

(6) (a) Simoyan, V. V.; Hohnson, J. K.; Kuznetsova, A.; et al. *J. Chem. Phys*. **2001**, *114*, 4180. (b) Kimoto, Y.; Mori, H.; Mikami, T.; et al. *Jpn. J. Appl. Phys., Part 1* **2005**, *44*, 1641. (c) Yu, W.; Wang, X. X.; Ni, X. G.; et al. *Chin. J. Chem. Phys.* **2005**, *18*, 187. (d) Durbahc, S. H.; Witcomb, M. J.; Coville, N. *J. Fullerenes Nanotubes Carbon Nanostruct.* **2005**, *13*, 155.

(7) (a) Scrivens, W. A.; Tour, J. M. *J. Chem. Soc., Chem. Commun*. **1993**, 1207. (b) Ruoff, R. S.; Tse, D. S.; Malhotra, R.; Lorents, D. C. *J. Phys. Chem.* **1993**, *97*, 3379. (c) Jung, S. K.; Chae, Y. R.; et al. *J. Microbiol. Biotechnol*. **2005**, *15*, 234, (d) Wu, X. F.; Shi, G. Q. *J. Mater. Chem.* **2005**, *15*, 1833. (e) Borondics, F.; Bokor, M.; Matus, P.; et al. *Fullerenes Nanotubes Carbon Nanostruct.* **2005**, *13*, 375. (f) Ramanathan, T.; Fisher, F. T.; Ruoff, R. S.; et al. *Chem. Mater*. **2005**, *17*, 1290. (g) Chopra, N.; Majumder, M.; Hinds, B. *J. Adv. Funct. Mater*. **2005**, *15*, 858. (h) Xie, H.; Ortiz-Acevedo, A.; Zorbas, V.; et al. *J. Mater. Chem.* **2005**, *15*, 1734.

(8) (a) Peralta-Inga, Z.; Lane, P.; Murray, J. S.; Boyd, S.; Grice, M. E.; O'Conor, C. J.; Politzer, P. *Nano Lett.* **2003**, *3*, 21. (b) Tournus, F.; Charlier, J. C. *Phys. Rev. B* **2005**, *71*, 165421. (c) Shang, H. Y.; Liu, Ch. G.; Chai, Y. M.; Xing, J. X. *Acta Chim. Sin.* **2004**, *62*, 888.

(9) Parr, R. G.; Yang, W. *Density Functional Theory of Atoms and Molecules*; Oxford University Press: Oxford, UK, 1989.

(10) Sen, K. D. *Eletronegativity*; Structure and Bonding, No. 66; Springer-Verlag: New York, 1987.

(11) Sen, K. D. *Chemical Hardness*; Structure and Bonding, No. 80; Springer-Verlag: New York, 1993.

(12) Parr, R. G.; Yang W. *J. Am. Chem. Soc*. **1984**, *106*, 4049.

(13) Yang, W.; Parr, R. G. *Proc. Natl. Acad. Sci. U.S.A.* **1985**, *82*, 6723.

(14) Pauling, L. *The Nature of the Chemical Bound*; Cornell University Press: Ithaca, NY, 1960.

(15) (a) Pearson, R. G. *Hard and Soft Acids and Bases*; Dowden, Hutchinson and Ross: Stroudsberg, PA, 1973; (b) Pearson R. G. *J. Am. Chem. Soc.* **1963**, *85*, 3533.

(16) Pearson, R. G. *J. Chem. Educ*. **1987**, *64*, 561.

(17) (a) Pearson, R. G. *Chemical Hardness*: *Applications from Molecules to Solids*; Wiley-VCH Verlag GMBH: Weinheim, Germany, 1997. (b) Pearson, R. G. *Acc. Chem. Res.* **1993**, *26*, 250.

(18) (a) Parr, R. G.; Chattaraj, P. K. *J. Am. Chem. Soc.* **1991**, *113*, 1854. (b) Chattaraj, P. K.; Liu, G. H.; Parr, R. G. *Chem. Phys. Lett*. **1995**, *237*, 171.

(19) Chattaraj, P. K. *Proc. Indian Natl. Sci. Acad., Part A* **1996**, *62*, 1133.

(20) Ayers, P. W.; Parr, R. G. *J. Am. Chem. Soc*. **2000**, *122*, 2010.

(21) Chattaraj, P. K.; Poddar, A. *J. Phys. Chem. A*. **1998**, *102*, 9944. Chattaraj, P. K.; Poddar, A. *J. Phys. Chem. A.* **1999**, *103*, 1274.

(22) Chattaraj, P. K.; Poddar, A. *J. Phys. Chem. A* **1999**, *103*, 8691.

(23) Parr, R. G.; Donnelly, R. A.; Levy, M.; Palke, W. E. *J. Chem. Phys.* **1978**, *68*, 3801.

(24) Parr, R. G.; Pearson, R. G. *J. Am. Chem. Soc*. **1983**, *105*, 7512.

(25) Parr, R. G.; Szentpály, L.; Liu, S. *J. Am. Chem. Soc*. **1999**, *121*, 1922.

(26) Godbout, N.; Salahub, D. R.; Andzelm, J.; Wimmer, E. *Can. J. Phys.* **1992**, *70*, 560.

(27) Becke, A. D. *Phys. Rev. A* **1988**, *38*, 3098.

(28) (a) Lee, C.; Yang, W.; Parr, R. G. *Phys. Rev. B* **1988**, *37*, 785. (b) Colle, R.; Salvetti, D. *Theor. Chim. Act* **1975**, *37*, 329. (c) Colle, R.; Salvetti, D. *J. Chem. Phys.* **1983**, *79*, 1404.

(29) Koopmans, T. A. *Physical* **1933**, *1*, 104.

(30) Koster, A. M.; Flores-Moreno, R.; Geudtner, G.; Goursot, A.; Heine, T.; Reveles, J. U.; Vela, A.; Salahud, D. R. *deMon 2003*; NRC: Canada, 2003.

(31) Schaftenaar, G.; Noordik, J. H. Molden 4.3: a pre- and post-processing program for molecular and electronic structures. *J. Comput.-Aided Mol. Design* **2000**, *14*, 123.

(32) *GaussView*, 3.07; Gaussian Inc.: Carnegie Office Park Bldg. 6, Pittsburgh, PA, 2003.

(33) Saito, R.; Dresselhaus, G.; Dresselhaus, M. S. *Physical Properties of Carbon Nanotubes*; Imperial College Press: London, UK, 2001.

(34) (a) Majumder, Ch.; Briere, T. M.; Mizuseki, H.; Kawazoe, Y. *J. Chem. Phys.* **2002**, *117*, 2819. (b) Krasheninnikov, A. V.; Nordlund, K.; Lehtinen, P. O.; Foster, A. S.; Ayuela, A.; Nieminen, R. M. *Phys.* Rev. *B* **2004**, *69*, 073402.